Published in final edited form as:
Invest Ophthalmol Vis Sci. 2009 August ; 50(8): 3977–3984. doi:10.1167/iovs.08-2910.

The Effects of Transient Retinal Detachment on Cavity Size and Glial and Neural Remodeling in a Mouse Model of X-Linked Retinoschisis

Gabriel Luna[1,2], **Sten Kjellstrom**[3,4], **Mark R. Verardo**[1,2], **Geoffrey P. Lewis**[1,2], **Jiyun Byun**[2], **Paul A. Sieving**[3], and **Steven K. Fisher**[1,2,5]

[1]Neuroscience Research Institute, University of California Santa Barbara, Santa Barbara, California [2]Center for Bioimage Informatics, University of California Santa Barbara, Santa Barbara, California [3]National Eye Institute/NIDCD, National Institutes of Health, Bethesda, Maryland [4]Department of Ophthalmology, Wallenberg Retina Center, University of Lund, Lund, Sweden [5]Department of Molecular, Cellular, and Developmental Biology, University of California Santa Barbara, Santa Barbara, California

Abstract

Purpose—To determine the cellular consequences of retinal detachment in retinoschisin knockout (*Rs1*-KO) mice, a model for retinoschisin in humans.

Methods—Experimental retinal detachments (RDs) were induced in the right eyes of both *Rs1*-KO and wild-type (wt) control mice. Immunocytochemistry was performed on retinal tissue at 1, 7, or 28 days after RD with antibodies to anti-GFAP, -neurofilament, and -rod opsin to examine cellular changes after detachment. Images of the immunostained tissue were captured by laser scanning confocal microscopy. Quantitative analysis was performed to measure the number of Hoechst-stained photoreceptor nuclei and their density, number, and size of inner retinal cavities, as well as the number of subretinal glial scars.

Results—Since detachments were created with balanced salt solution, by examination, all retinas had spontaneously reattached by 1 day. Cellular responses common to many photoreceptor degenerations occurred in the nondetached retinas of *Rs1*-KO mice, and, of importance, RD did not appear to significantly accentuate these responses. The number of schisis cavities was not changed after detachment, but their size was reduced.

Conclusions—These data indicate that large short-term RD in *Rs1*-KO mice, followed by a period of reattachment may cause a slight increase in photoreceptor cell death, but detachments do not accentuate the gliosis and neurite sprouting already present and may in fact reduce the size of existing retinal cavities. This finding suggests that performing subretinal injections to deliver therapeutic agents may be a viable option in the treatment of patients with retinoschisis without causing significant cellular damage to the retina.

X-linked juvenile retinoschisis (XLRS) (*schisis* the Greek word meaning splitting or separation) is a genetically recessive inherited type of retinal degeneration that results in the delamination of inner retinal layers and the formation of cavities within the retina. Although

Corresponding author: Steven K. Fisher, Neuroscience Research Institute, University of California Santa Barbara, Santa Barbara, CA 93106-5060; fisher@lifesci.ucsb.edu.

Disclosure: G. Luna, None; S. Kjellstrom, None; M.R. Verardo, None; G.P. Lewis, None; J. Byun, None; P.A. Sieving, None; S.K. Fisher, None;

the X-linked genetic mode of inheritance primarily affects males, homozygous females affected with X-linked retinoschisis manifest similar phenotypic characteristics.[1] XLRS is the most frequent form of juvenile macular degeneration among males and is typically diagnosed during preadolescence, often as a consequence of academic shortcomings, specifically reading impairments.[2] The prevalence of males with this disease has been estimated to range from 1 in 5,000 to 1 in 25,000.[2] In the clinical setting, XLRS is characterized by the disorganization of the inner retinal layers where many microcystic cavities are present when viewed by funduscopy or optical coherence tomography (OCT).[3,4]

The cause of XLRS has been linked to mutations in the gene encoding retinoschisin (RS), a 24-kDa secreted protein found in the retina[5] and pineal gland.[6] The retinoschisin molecule contains a conserved discoidin domain (DD)[5] and is a member of the DD family of proteins that are involved in cell adhesion and cell– cell interactions.[7–10] Retinoschisin is expressed early in the development of the mouse retina, and all retinal neurons express RS after differentiation, beginning with the ganglion cells followed by the more distal neurons.[6,11] After the retina reaches maturity, RS is mainly expressed in the outer half of the inner nuclear layer (INL) and by photoreceptor inner segments, but also continues to be expressed in all classes of retinal neurons although to a lesser degree.[6]

Currently, more than 170 disease-causing mutations have been identified in the *RS1* gene (RetinoschisisDB; http://www.dmd.nl/rs/index.html/ provided in the public domain by Leiden University Medical Center, Leiden, The Netherlands), with missense mutations being the majority followed by frame-shift, nonsense, and point mutations, deletions, and insertions. All these mutations show similar phenotypes with the splitting of the retina, formation of stereotypical large cavities in the inner retina, and an affected ERG.[8,12]

XLRS can also give rise to several severe complications, including peripheral schisis,[13] vitreous hemorrhaging, neovascular glaucoma, atrophy of the retinal pigment epithelium (RPE), and in advanced cases, retinal detachment as well as proliferative vitreoretinopathy (PVR).[8,14,15] Preadolescent patients with XLRS are usually examined, with funduscopy and OCT if available, on a yearly basis by their pediatric ophthalmologist, and less frequently at older ages. Because of the fragility of retinas lacking retinoschisin[5,11] and the high incidence of retinal detachments in XLRS,[15,16] vitreous surgery is generally avoided and is considered complicated. A recent study, however, indicates that vitreous surgery may have a positive role in partially restoring visual acuity by relieving the vitreous traction in retinas with foveal schisis resulting in reattachment of the retina.[17]

Ultimately, 16% to 22% of patients with XLRS develop rhegmatogenous detachments (i.e., detachment with a retinal tear).[18,19] Retinal detachment in otherwise healthy eyes frequently results in diminished visual capacity in humans. Even after uncomplicated surgical reattachment, the recovery of vision can vary greatly.[20] It is estimated that, in 20% to 60% of the surgical population, visual acuity recovers to only approximately 20/50.

There are currently three mouse models of human XLRS, all of which display structural and functional features similar to human XLRS,[21–23] including a more affected b- than a-wave and splitting of multiple retinal layers with large intraretinal cavities. The greater reduction observed in the ERG b-wave suggests a disruption of synaptic transmission at the photoreceptor/bipolar cell synapse in the absence of retinoschisin protein. These *Rs1*-knockout (KO) mice have been important in the understanding and development of therapies for human XLRS. Ocular gene therapy, delivered either in the subretinal space or in the vitreous, is one such treatment that has been evaluated in the XLRS mouse model with promising results.[22,24,25] Traditionally, ocular gene therapy has involved delivering a small amount of fluid (1–2 μL) carrying the replacement gene vector into the subretinal space, where the target is both the

inner and outer retina.[26] Intravitreal delivery of the vector is an efficient administration route in the *Rs1*-KO mouse model, promoting restoration of retinal architecture and closing of cavities, preservation of photoreceptors, and functional rescue[22] with improvement in ERG.[25] In an important finding for treating human disease, recent studies in the *Rs1*-KO mouse have demonstrated that such gene therapy is able to restore a functional ERG b-wave during late stages of the disease.[25,27]

Recent clinical phase 1 gene therapy trials for human retinal degeneration in Leber congenital amaurosis (LCA) show promising results.[28,29] Delivering the gene vector in the subretinal space produced a short-lived retinal detachment with no signs of retinal damage due to the procedure. In XLRS, with a particularly fragile retina prone to detachment, the question remains whether physical trauma caused by subretinal intervention will accentuate the cellular damage already present in retinas affected by retinoschisis. In one study, using wild-type (wt) mice aiming to identify genes involved in retinal detachment and subsequent reattachment, the *Rs1* gene was upregulated as early as 2 hours after detachment and thought to be involved in the physical cohesion of the retina.[30]

Two studies in recent years have shown that various cell types of the mouse retina alter their morphology and become reactive in response to retinal detachment.[31,32] It is important to note that these previous studies were performed with a solution of sodium hyaluronate (Healon; Pharmacia & Upjohn, Uppsala, Sweden), to produce sustained long-term retinal detachments. In contrast, we used injections of balanced salt solution (BSS; Alcon, Ltd., Fort Worth, TX) to create short-lived retinal detachments that more closely mimic the transient detachment that occurs as a result of gene therapy. We show here that a brief detachment interval (~ 1 day), even though large in size, does not increase damage to the retina out to 28 days later and may in fact reduce the size of the existing cavities.

Materials and Methods

Animals

Rs1-KO ($Rs1^{-/y}$) mice were generated from C57BL/6 blastocytes, and the mice were backcrossed more than 10 generations, as described elsewhere.[22,25] All mice, C57BL/6 wt ($Rs1^{+/y}$) and *Rs1*-KO were 2 months of age at the beginning of the study. Three *Rs1*-KO mice and three littermate wt mice from each time point were used for immunocytochemical studies. The animal experiments were conducted in accordance with the National Institutes of Health (NIH) Animal Care and Use Committee protocols, the ARVO Statement for the Use of Animals in Ophthalmic and Vision Research, and the guidelines of the Animal Resource Center of the University of California Santa Barbara (Santa Barbara, CA).

Transient Experimental Retinal Detachment

Retinal detachments were produced in the right eyes of *Rs1*-KO and C57BL/6J (wt) mice, and left eyes served as the control. First, a pilot hole was created with a 30-gauge needle through the sclera a few millimeters below the limbus. A fine custom-pulled glass micropipette was then introduced transvitreously and inserted between the neural retina and the RPE, at which time approximately 5 μL of balanced salt solution was infused, detaching approximately 75% of the retina. A glass coverslip, placed on the cornea, was used to visualize the retina during surgery. Since the glass pipette tip (~ 1 cm long) was very thin and flexible, it did not penetrate or damage the lens; no cataracts were observed at the time of euthanization. The mice were euthanized at 1, 7, or 28 days after detachment. A 1-day animal is considered to have had a detached retina for the majority of the 24-hour period. As described in the Results section, since balanced salt solution was used to create the detachments, the retinas spontaneously reattached by 24 hours; hence, a 7-day animal is considered detached for 1 day and reattached

for 6 days. Similarly, a 28 day detachment is considered having a 1-day retinal detachment followed by a reattachment period of 27 days.

Tissue Preparation

After euthanatization, the eyes were first lightly cauterized to mark the hemisphere where the detachment originated (i.e., the region where the tip penetrated the retina). The eyes were then enucleated and immersion fixed overnight in 4% paraformaldehyde in sodium cacodylate buffer (0.1 M; pH 7.4) at 4°C. The next day the cornea and lens were removed to form an eyecup which was then bisected through the area of detachment. Sections were cut transversely through the bisected area of detachment.

Immunocytochemistry

Immunocytochemistry was performed, as described previously.[32] Briefly, the eyes were rinsed in phosphate-buffered saline (PBS; pH 7.4) three times for 15 minutes each and one time for 60 minutes, embedded in low-melt agarose (5%; Sigma-Aldrich, St. Louis, MO) at 45°C and subsequently sectioned at 100 μm using a vibratome (Leica, Lumberton, NJ). To prevent nonspecific binding of antibodies, the reactions in the retinal sections were blocked overnight with normal donkey serum 1:20 in PBS containing 0.5% BSA, 0.1% Triton X-100, and 0.1% Azide (PBTA) at 4°C on a rotator for continuous agitation. After the overnight blocking step, the PBTA was removed and primary antibodies, diluted in PBTA, were added for another overnight incubation at 4°C. The next day retinal sections were rinsed in PBTA, three times for 15 minutes each and one time for 60 minutes at which time the corresponding secondary antibodies were added for the last overnight incubation at 4°C. Antibodies to the following proteins were used: glial fibrillary acidic protein (GFAP) (1:400, rabbit polyclonal, DAKO, Carpinteria, CA), rod opsin (1:500, mouse monoclonal; a gift from Robert S. Molday, University of British Columbia, Vancouver), and neurofilament protein (1:500, mouse monoclonal; Biomeda, Hayward, CA). The secondary antibodies included donkey-anti mouse, goat, or rabbit conjugated to Cy2, Cy3, or Cy5 (Jackson ImmunoResearch, Laboratories, West Grove, PA). Finally, the sections were rinsed in PBTA as just described, mounted in 5% *n*-propyl gallate in glycerol on glass slides, covered with a coverslip, and subsequently sealed with nail polish. In some cases, the sections were mounted in *n*-propyl gallate containing the nuclear stain Hoechst (1:5000; Molecular Probes, Eugene, OR). The specimens were viewed and images collected with a laser scanning confocal microscope (FluoView 500; Olympus Center Valley, PA). *Rs1*-KO and control eyes from the same immunohistochemistry experiment were viewed during the same session, with black and gain levels kept constant to allow for comparisons and semiquantitation of labeling intensity.

Quantification

The number of photoreceptor cells (i.e., number of nuclei/area of ONL) and schisis cavities, and the size of the schisis cavities relative to the area of the INL were all calculated from 50 to 100 randomly collected confocal images at a resolution of 512 by 512 with a pixel size of 0.62 μm. These images were taken from the central to the midperipheral retina in each of the relevant animals (schisis cavities do not exist in wt mice). The number of photoreceptor nuclei was counted in the images with an automated computer program (Nucleus Detector, provided in the public domain at http://www.bioimage.ucsb.edu, Center for Bioinformatics, University of California at Santa Barbara).[33] The area of the ONL within each image was also automatically calculated using the method previously described.[34] An average density of photoreceptors for all the animals within a group was then calculated using the average density per animal. To determine the number and area of the schisis cavities, borders were manually drawn around the cavities on the digital images (DminViewer software; http://dimin.m6.net/software/viewer/ developed and provided in the public domain by Dimitry

V. Federov under the auspices of several grantors). The average number of schisis cavities was calculated per millimeter of INL for each group of *Rs1*-KO animals. The area of the schisis cavities within an image was calculated by measuring the area of the cavities/the area of the INL × 100 to give a percentage of INL area occupied by the cavities. These areas were averaged as described for photoreceptor cell counts to provide an overall average for each group. For statistical purposes, $P > 0.05$ was not considered statistically significant.

Determining a representative number for subretinal scars in the various samples was done somewhat differently in an attempt to avoid bias in selecting areas that have scars and yet assure that enough sampling area was obtained to allow for some measure of significance. In this case, central-to-peripheral retinal mosaics approximately 2 mm in length were constructed from one animal from the wt control, wt 7-day detached, *Rs1*-KO control, and *Rs1*-KO 7-day detached groups. There are no subretinal scars in the wt control animals. The data are presented as the number of scars per millimeter within the retinal mosaics.

Results

Retinal Reattachment

In previous studies we used a dilute solution of 0.25% sodium hyaluronate (Healon; Pharmacia & Upjohn, Uppsala, Sweden) to maintain detachments for a long period (e.g., months).[32] In this study, we created large detachments with balanced salt solution and under these circumstances we observed that the retina of both wt and *Rs1*-KO reattaches within 24 hours. These results are similar to those shown by Nour et al.[35] who created small retinal blebs by injecting 1 μL of saline into the subretinal space.

Müller Cell Reactivity

In the *Rs1*-KO control eyes, there was a much greater expression of the intermediate filament protein GFAP than in the wt control eyes; anti-GFAP labeling of Müller cells extended from the ILM through the ONL in the *Rs1*-KO (Fig. 1C) whereas no Müller cell labeling was detected in the wt retinas (Fig. 1A). After detachment in wt animals at the 28-day time point (i.e., 1-day detached, 27-day reattached), anti-GFAP labeling had increased slightly in the Müller cells (Fig. 1B), but the labeling was still less than that observed in nondetached *Rs1*-KO eyes (Fig. 1C). No apparent difference in anti-GFAP labeling was observed between *Rs1*-KO detached (Fig. 1D) and nondetached retinas at any time point. Anti-GFAP expressed by astrocytes also appeared similar in all animals and did not vary between wt and *Rs1*-KO or between attached and detached retinas (Fig. 1).

It has been shown previously that detachment of the wt mouse retina using sodium hyaluronate to maintain the detachment for 7 days leads to Müller cell hypertrophy and growth past the outer limiting membrane (OLM) forming subretinal scars.[32] In our study, scars formed by Müller cells were observed in control *Rs1*-KO retinas, and they continued to be present after detachment, even though retinas had reattached by day 1 (Figs. 1C, 1D). A hemisection of an attached *Rs1*-KO retina shows several anti-GFAP-stained processes extending past the OLM where they disrupt the outer segment layer (Fig. 2A, arrows). A higher magnification view of similar areas (Figs. 2B–D) reveals these glial processes labeled by anti-GFAP (green) to have a complex morphology with a tangled appearance similar to that of subretinal scars in mice,[32] cats,[36] and humans[37] after detachment. The morphology of these glial processes in detached and nondetached *Rs1*-KO retinas appeared the same as those observed in the detached wt retinas.[32]

The prevalence of GFAP-positive processes crossing the OLM into the subretinal space was determined from mosaiced adjacent images from individual retinas as described previously.

[38] The number of scars was similar in the *Rs1*-KO detached (3.47/mm) and nondetached (3.40/mm) retinas and more than double the number than in wt detached retinas in the same respective experimental group (1.5/mm) indicating that detachment did not increase the number of subretinal scars in the *Rs1*-KO retinas (Fig. 3; 7-day time point).

Schisis Cavities

The most prominent phenotypic feature of these *Rs1*-KO animals is the appearance of schisis cavities (Figs. 1C, 2D).[22,25] Images from laser scanning confocal microscopy were used to quantitate the number of cavities/mm in detached and nondetached *Rs1*-KO retinas (Fig. 4). The number of cavities was significantly increased at 1 day of detachment but then decreased as the retina was reattached for longer periods of time so that their number did not show a statistically significant difference between the *Rs1*-KO control and the 7 or 28 day groups (Fig. 4). However, there were significant differences in the area of the inner retina covered by the schisis cavities for the detached and nondetached *Rs1*-KO eyes (Fig. 5). The area of the schisis cavities was consistently smaller overall in the detached *Rs1*-KO eyes when compared with the nondetached controls. The effect created a decrease in the average area of the INL occupied by schisis cavities from 17.48% in the *Rs1*-KO nondetached eyes to approximately 8.46% in the 28-day *Rs1*-KO animals.

Photoreceptors

Both nondetached and detached *Rs1*-KO retinas displayed focal regions of outer segment disruption and associated rod opsin redistribution adjacent to the subretinal scars (Figs. 2B, 2C). Photoreceptor cell bodies were present in the subretinal space within areas of the glial scars (Fig. 2D; arrow) in both attached and detached *Rs1*-KO retinas. Rod opsin redistribution to the ONL was not observed in wt detached retinas, most likely because of the very brief period of detachment.

To establish the magnitude of cell death occurring in the eyes, the density of photoreceptor cells (number of cells/mm^2) was determined from retinal images using an automated cell counting program.[34] Since we did not observe a decline in photoreceptor number in the left (unoperated control) eyes of the *Rs1*-KO mice over the 1 month of this experiment, the ONL cell counts from those eyes were pooled to give an overall average of photoreceptor density in the *Rs1*-KO eyes (percentage of photoreceptor cell density is shown as a percentage of values in control animals in Fig. 6). Cell counts from the left eyes of the wt control retinas were similarly pooled. The average cell densities were 51,764 ± 3,483 cells/mm^2 in wt animals and 49,976 ± 3,027 cells/mm^2 in the *Rs1*-KO nonsurgical eyes. These data represent a difference of 3% and although small, show statistical significance when analyzed with a Student's *t*-test ($P < 0.01$). The slight decline in cell density in the wt mice in the 28-day experiment to an average of 50,844 ± 1,952 cells/mm^2 does not show statistical significance. Although the decrease in photoreceptor cells in the *Rs1*-KO animals over the course of the study is small (Fig. 6), the change between control 49,976 ± 3,027 cells/mm^2 and 28 day animals 47,855 ± 2,276 cells/mm^2 is statistically significant $P < 0.0001$.

Neurite Outgrowth

It has been observed that retinas reacting to the loss of photoreceptor cells contain neurite processes that originate from both rod bipolar and horizontal cells, and most often grow into the ONL adjacent to a glial scar but sometimes into the inner retina as well.[32,36,37,39–42] A recent study by Takada et al.[43] also demonstrated neurite outgrowth from both rod bipolar and horizontal cells in *Rs1*-KO mice.[43] Positive neurofilament processes indicative of neurite outgrowth were observed extending into the inner (Figs. 7A, 7B, arrows) and outer retina (Figs. 7C–E) in all *Rs1*-KO mice. These processes were similar in appearance to those observed in wt mouse retina after 7 days of detachment,[32] and they were morphologically consistent with

processes arising from horizontal cells. Although the infrequency of these extensions made quantification difficult, our observations suggest strongly that there was no difference in the size or frequency of neurites in the *Rs1*-KO retinas whether detached or not. Double labeling experiments with anti-neurofilament and anti-GFAP suggest a clear morphologic association of neurites with reactive Müller cell processes growing past the OLM (Figs. 7D, 7E arrowheads).[36]

Discussion and Conclusions

In this study, we showed that features common to both inherited photoreceptor degeneration and retinal detachment (i.e., the loss of photoreceptors, glial reactivity, and neuronal remodeling)[42,44] occur in a mouse model of X-linked retinoschi-sis. Short-term retinal detachment resulted in no obvious exacerbation of gliosis or neurite sprouting, although it may have caused a slight increase in photoreceptor cell death. However, there was a clear effect observed in the size of the schisis cavities which decreased in the detached retinas from approximately 17% to 8% of the INL area respectively in control animals and in the 28-day experimental eyes. Both the nondetached *Rs1*-KO retinas and those with retinal detachment exhibited similar signs of retinal trauma as shown by an upregulation in the expression of the intermediate filament protein GFAP, a common marker for neurotrauma. These findings suggest that the defective RS protein caused retinas from *Rs1*-KO animals to be in a state of cellular reactivity before detachment. Indeed, glial scar formation in the subretinal space, often accompanied by neurite outgrowth from horizontal cells, was under way in the *Rs1*-KO mice without detachment. Thus, humans with X-linked retinoschisis may have a slow, ongoing formation of subretinal scar tissue. This is not a benign event, since in areas with subretinal growth there was outer segment disruption, rod opsin redistribution, and extrusion of photoreceptor nuclei into the subretinal space. Moreover, it has been shown that the presence of a subretinal glial scar prevents regeneration of outer segments.[45] Since glial scars can have detrimental effects on photoreceptor health, the data suggest that therapy to treat the RS defect may also benefit from treatment that reduces the severity of reactive gliosis. Unfortunately, there are presently no treatments for this condition. On the other hand, subretinal glial scar formation was not accentuated by short-term retinal detachment, indicating that subretinal gene therapy may not exacerbate the glial reactivity already present in patients with X-linked retinoschisis.

Transient detachments did not induce a significant loss of photoreceptors in the wt animals but did cause a slight (3%) decline in photoreceptor cell density in the fragile *Rs1*-KO retinas after 28 days. This decline is small and may represent the fact that these detachments were large, encompassing ~75% of the retina. Thus, cell death may not be a concern in the case of small retinal blebs created for gene therapy; although in practice the bleb would be located near to the macula, which is most critical for visual function. The results though, may indicate a greater susceptibility of patients with retinoschisis to the effects of a large rhegmatogenous detachment than observed in the general population.

While there was a slight increase in the number of inner retinal cavities 1 day after detachment, during which time the retina was mostly detached, this number decreased to the level of the nondetached retinas after reattachment at 7 and 28 days. Also, the physical area of the INL occupied by the cavities decreased in the detached retinas. It has been reported that stressing or injuring the eye can have a profound effect on the osmotic state of the retina.[46] A similar phenomenon may occur here where detachment induces a hyperactivation of channel mediated movements of potassium and water by Müller cells that affect the inner retinal layers where these cavities exist. Clearly, this effect was relatively long-lived in the mice, since it was apparent in the animals 27 days after a 1-day detachment.

Although studies in mice have demonstrated that restoring RS protein production rescues the phenotype of this disease,[25] further examination of other cellular events under way before the application of gene therapy may prove crucial in developing a more complete and long-term treatment for patients affected by XLRS. Indeed, subretinal glial scar formation and neurite sprouting seem to be as characteristic as the splitting of the retinal layers and loss of photoreceptor cells in the *Rs1*-KO retinas. Disturbance of the retina by any subretinal route of gene therapy in these patients is likely to be inevitable, and given the fragility of these retinas and their propensity for retinal detachment, this possibility must be taken seriously. Our results are encouraging, although a reduction in the size of schisis cavities by transient retinal detachment could partially confound the outcome of a clinical trial using this approach, possibly masking the benefits of gene therapy.[17]

Acknowledgments

The authors thank Ronald Bush for a valuable critique of our manuscript, as well as Cali Johnson for technical assistance.

Supported in part by research Grant EY-000888 (SKF) from the National Eye Institute, National Institutes of Health; Grants ITR-0331697 and IIS-0808772 (SKF) from the National Science Foundation; the National Institutes of Health, Intramural Research Program (PAS); and NCRR Shared Instrumentation Grant 1S10RR017753-01.

References

1. Rodriguez FJ, Rodriguez A, Mendoza-Londono R, Tamayo ML. X-Linked retinoschisis in three females from the same family: a phenotype-genotype correlation. Retina 2005;25:69–74. [PubMed: 15655444]
2. George ND, Yates JR, Moore AT. X linked retinoschisis. Br J Ophthalmol 1995;79:697–702. [PubMed: 7662639]
3. Azzolini C, Pierro L, Codenotti M, Brancato R. OCT images and surgery of juvenile macular retinoschisis. Eur J Ophthalmol 1997;7:196–200. [PubMed: 9243227]
4. Prenner JL, Capone A Jr, Ciaccia S, Takada Y, Sieving PA, Trese MT. Congenital X-linked retinoschisis classification system. Retina 2006;26:S61–S64. [PubMed: 16946682]
5. Sauer CG, Gehrig A, Warneke-Wittstock R, et al. Positional cloning of the gene associated with X-linked juvenile retinoschisis. Nat Genet 1997;17:164–170. [PubMed: 9326935]
6. Takada Y, Fariss RN, Tanikawa A, et al. A retinal neuronal developmental wave of retinoschisin expression begins in ganglion cells during layer formation. Invest Ophthalmol Vis Sci 2004;45:3302–3312. [PubMed: 15326155]
7. Vogel W. Discoidin domain receptors: structural relations and functional implications. FASEB J 1999;13(suppl):S77–S82. [PubMed: 10352148]
8. Tantri A, Vrabec TR, Cu-Unjieng A, Frost A, Annesley WH, Don-sono LA. X-Linked retinoschisis: a clinical and molecular genetic review. Surv Ophthalmol 2004;49:214–230. [PubMed: 14998693]
9. Vijayasarathy C, Gawinowicz MA, Zeng Y, Takada Y, Bush RA, Sieving PA. Identification of two mature isoforms of retinoschisin in murine retina. Biochem Biophys Res Commun 2006;349:99–105. [PubMed: 16930543]
10. Vijayasarathy C, Takada Y, Zeng Y, Bush RA, Sieving PA. Retinoschisin is a peripheral membrane protein with affinity for anionic phospholipids and affected by divalent cations. Invest Ophthalmol Vis Sci 2007;48:991–1000. [PubMed: 17325137]
11. Molday LL, Hicks D, Sauer CG, Weber BHF, Molday RS. Expression of X-linked retinoschisis protein RS1 in photoreceptor and bipolar cells. Invest Ophthalmol Vis Sci 2001;42:816–825. [PubMed: 11222545]
12. Sikkink SK, Biswas S, Parry NR, Stanga PE, Trump D. X-linked retinoschisis: an update. J Med Genet 2007;44:225–232. [PubMed: 17172462]
13. Manchot WA. Pathology of hereditary juvenile retinoschisis. Arch Ophthalmol 1972;88:131–138. [PubMed: 5054298]

14. Deutman, AF. Macular dystrophies. In: Ryan, SJ.; Schachat, AP.; Murphy, RP., editors. Medical Retina. Vol. 2nd. Vol. 2. St. Louis, MO: Mosby; 1994. p. 1186-1240.
15. Kellner U, Brummer S, Foerster MH, Wessing A. X-linked congenital retinoschisis. Arch Clin Exp Ophthalmol 1990;228:432–437.
16. George ND, Yates JR, Moore AT. Clinical features in affected males with X-Linked retinoschisis. Arch Ophthalmol 1996;114:274–280. [PubMed: 8600886]
17. Ikeda F, Iida T, Kishi S. Resolution of retinoschisis after vitreous surgery in X-linked retinoschisis. Ophthalmology 2008;115:718–722.e1. [PubMed: 17854899]
18. Edwards, AO.; Robertson, JE. Basic Science and Inherited Retinal Disease. Vol. 4th. Ryan, SJ.; Hinton, DR., editors. Vol. 1. St Louis, MO: Elsevier, Mosby; 2006. p. 519-538.
19. Oh, KT.; Hartnett, ME.; Landers, MB. Retina. In: Ryan, SJ.; Wilkinson, CP., editors. Surgical Retina. Vol. 4th. Vol. 3. St Louis, MO: Elsevier, Mosby; 2006. p. 2013-2020.
20. Ross WH. Visual recovery after macula-off retinal detachment. Eye 2002;16:440–446. [PubMed: 12101451]
21. Weber BH, Schrewe H, Molday LL, et al. Inactivation of the murine X-linked juvenile retinoschisin gene, Rs1h, suggests a role of retinoschisin in retina cell layer organization and synaptic structure. Proc Natl Acad Sci USA 2002;99:6222–6227. [PubMed: 11983912]
22. Zeng Y, Takada Y, Kjellstrom S, et al. RS-1 Gene delivery to an adult Rs1h knockout mouse model restores ERG b-wave with reversal of the electronegative waveform of X-linked retinoschisis. Invest Ophthalmol Vis Sci 2004;44:3279–3285. [PubMed: 15326152]
23. Johnson BA, Ikeda S, Pinto LH, Ikeda A. Reduced synaptic vesicle density and aberrant synaptic localization caused by a splice site mutation in the Rs1h gene. Vis Neurosci 2006;23:887–898. [PubMed: 17266781]
24. Min S, Molday LL, Seeliger MW, et al. Prolonged recovery of retinal structure/function after gene therapy in an Rs1h-deficient mouse model of X-linked juvenile retinoschisis. Mol Ther 2005;12:644–651. [PubMed: 16027044]
25. Kjellstrom S, Bush RA, Zeng Y, Takada Y, Sieving PA. Retinoschisin gene therapy and natural history in the Rs1h-KO mouse: long term rescue from retinal degeneration. Invest Ophthalmol Vis Sci 2007;48:3837–3845. [PubMed: 17652759]
26. Hauswirth WW, Lewin AS. Ribozyme uses in retinal gene therapy. Prog Retin Eye Res 2000;19:689–710. [PubMed: 11029552]
27. Janssen A, Min SH, Molday LL, et al. Effect of late-stage therapy on disease progression in AAV-mediated rescue of photoreceptor cells in the retinoschisin-deficient mouse. Mol Ther 2008;6:1010–1017. [PubMed: 18388913]
28. Maguire AM, Simonelli F, Pierce EA, et al. Safety and efficacy of gene transfer for Leber's congenital amaurosis. N Engl J Med 2008;358:2240–2248. [PubMed: 18441370]
29. Bainbridge JW, Smith AJ, Baker SS, et al. Effect of gene therapy on visual function in Leber's congenital amaurosis. N Engl J Med 2008;358:2231–2239. [PubMed: 18441371]
30. Farjo R, Peterson WM, Naash MI. Expression profiling after retinal detachment and reattachment: a possible role for aquaporin-0. Invest Ophthalmol Vis Sci 2008;49:511–521. [PubMed: 18234993]
31. Nakazawa T, Takeda M, Lewis GP, et al. Attenuated glial reactions and photoreceptor degeneration after retinal detachment in mice deficient in glial fibrillary acidic protein and vimentin. Invest Ophthalmol Vis Sci 2007;48:2760–2768. [PubMed: 17525210]
32. Verardo MR, Lewis GP, Takeda M, et al. Abnormal reactivity of Müller cells after retinal detachment in mice deficient in GFAP and vimentin. Invest Ophthalmol Vis Sci 2008;49:3659–3665. [PubMed: 18469190]
33. Byun J, Verardo MR, Sumengen B, Lewis GP, Manjunath BS, Fisher SK. Automated tool for the detection of cell nuclei in digital microscopic images: application to retinal images. Mol Vis 2006;12:949–960. [PubMed: 16943767]
34. Byun, J.; Vu, N.; Sumengen, B.; Manjunath, BS. Proceedings of the IEEE International Symposium on Biomedical Imaging (ISBI). Crystal City, CA. New York: IEEE; 2006. Quantitative analysis of immunofluorescent retinal images; p. 1268-1271.

35. Nour M, Quiambao AB, Peterson WM, Al-Ubaidi MR, Naash MI. $P2Y_2$ Receptor agonist INS37217 enhances functional recovery after detachment caused by subretinal injection in normal and rds mice. Invest Ophthalmol Vis Sci 2003;44:4505–4514. [PubMed: 14507899]
36. Lewis, GP.; Fisher, SK. Retinal plasticity and Interactive cellular remodeling in retinal detachment and reattachment. In: Pinaud, R.; Tremere, LA.; Weerd, PD., editors. Plasticity in the Visual System: From Genes to Circuits. New York: Springer; 2006. p. 55-78.
37. Sethi CS, Lewis GP, Fisher SK, et al. Glial remodeling and neural plasticity in human retinal detachment with proliferative vitreoretinopathy. Invest Ophthalmol Vis Sci 2005;46:329–342. [PubMed: 15623793]
38. Byun, J.; Verardo, MR.; Vu, N., et al. Quantifying Structural Distortions in Retinal Tissue before and after Injury. Presented at the Workshop on Multiscale Biological Imaging, Data Mining and Informatics.; September 7-8, 2006; Santa Barbara, CA.
39. Lewis GP, Linberg KA, Fisher SK. Neurite outgrowth from bipolar and horizontal cells after experimental retinal detachment. Invest Ophthalmol Vis Sci 1998;39:424–434. [PubMed: 9478003]
40. Strettoi E, Prociatti V, Falsini B, Pignatelli V, Rossi C. Morphological and functional abnormalities in the inner retina of the rd/rd mouse. J Neurosci 2002;22:5492–5504. [PubMed: 12097501]
41. Strettoi E, Pignatelli V, Rossi C, Prociatti V, Falsini B. Remodeling of second-order neurons in the retina of rd/rd mutant mice. Vis Res 2003;43:867–877. [PubMed: 12668056]
42. Marc RE, Jones BW, Watt CB, Sterttoi E. Neural remodeling in retinal degeneration. Prog Retin Eye Res 2003;22:607–655. [PubMed: 12892644]
43. Takada Y, Vijayasarathy C, Zeng Y, Kjellstrom, Bush RA, Sieving PA. Synaptic pathology in retinoschisis knockout ($Rs1^{-/y}$) mouse retina and modification by rAAV-Rs1 gene delivery. Invest Ophthalmol Vis Sci 2008;49:3677–3686. [PubMed: 18660429]
44. Fisher SK, Lewis GP, Linberg KA, Verardo MR. Cellular remodeling in mammalian retina: results from studies of experimental retinal detachment. Prog Retin Eye Res 2005;24:395–431. [PubMed: 15708835]
45. Anderson DH, Guerin CJ, Erickson PA, Stern WH, Fisher SK. Morphological recovery in the reattached retina. Invest Ophthalmol Vis Sci 1986;27:184–187. [PubMed: 2417981]
46. Iandiev I, Pannicke T, Hollborn M, et al. Localization of glial aquaporin-4 and Kir4.1 in the light-injured murine retina. Neurosci Lett 2008;434:317–321. [PubMed: 18328627]

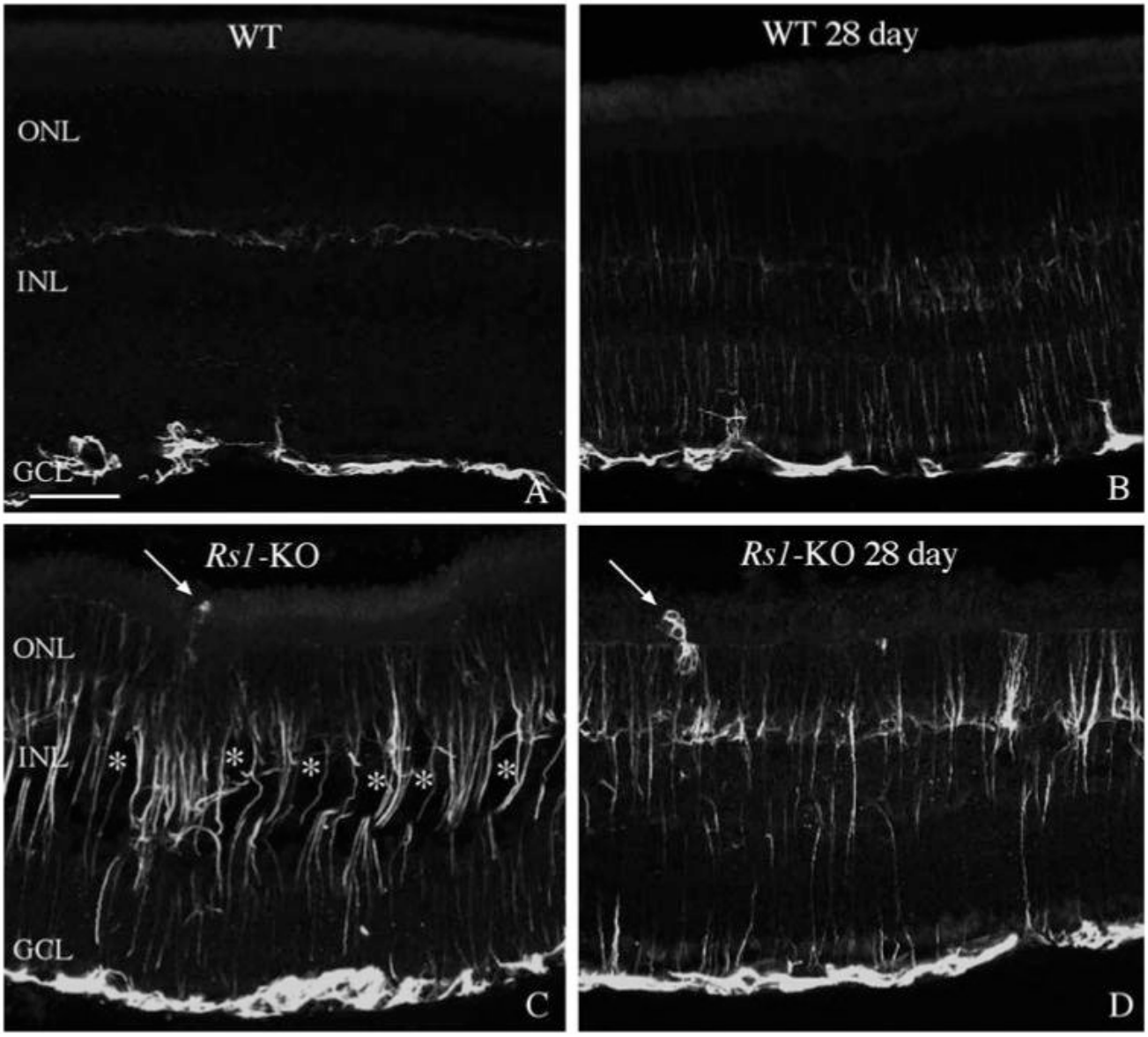

Figure 1.

Laser scanning confocal images comparing anti-GFAP labeling of Müller cells in wt nondetached and detached retinas (**A**, **B**) with *Rs1*-KO nondetached and detached retinas (**C**, **D**). In nondetached wt retinas, anti-GFAP labeled only astrocytes in the inner retina (**A**). After a 1-day detachment and 27 days of reattachment, anti-GFAP labeling slightly increased in the Müller cells and extended into the outer nuclear layer (ONL; **B**). In nondetached *Rs1*-KO retinas, anti-GFAP labeling of Müller cells extended throughout the entire retina and into the subretinal space (**C**; *arrow*). This pattern of labeling appeared similar in *Rs1*-KO animals after a 1-day detachment and 27 days of reattachment (**D**; *arrow* points to a subretinal glial scar.) Faint anti-GFAP labeling of horizontal cells was often visible in the outer plexiform layer (faint labeling in the *center* of Fig. 1A). This labeling was variable and did not increase after detachment; and it was usually obscured by the upregulation of GFAP in Müller cells. The cavities (✻) present in the detached *Rs1*-KO retina, appeared somewhat reduced in size

compared with the size in the nondetached *Rs1*-KO retina. INL, inner nuclear layer; GCL, ganglion cell layer. Scale bar: 50 μm.

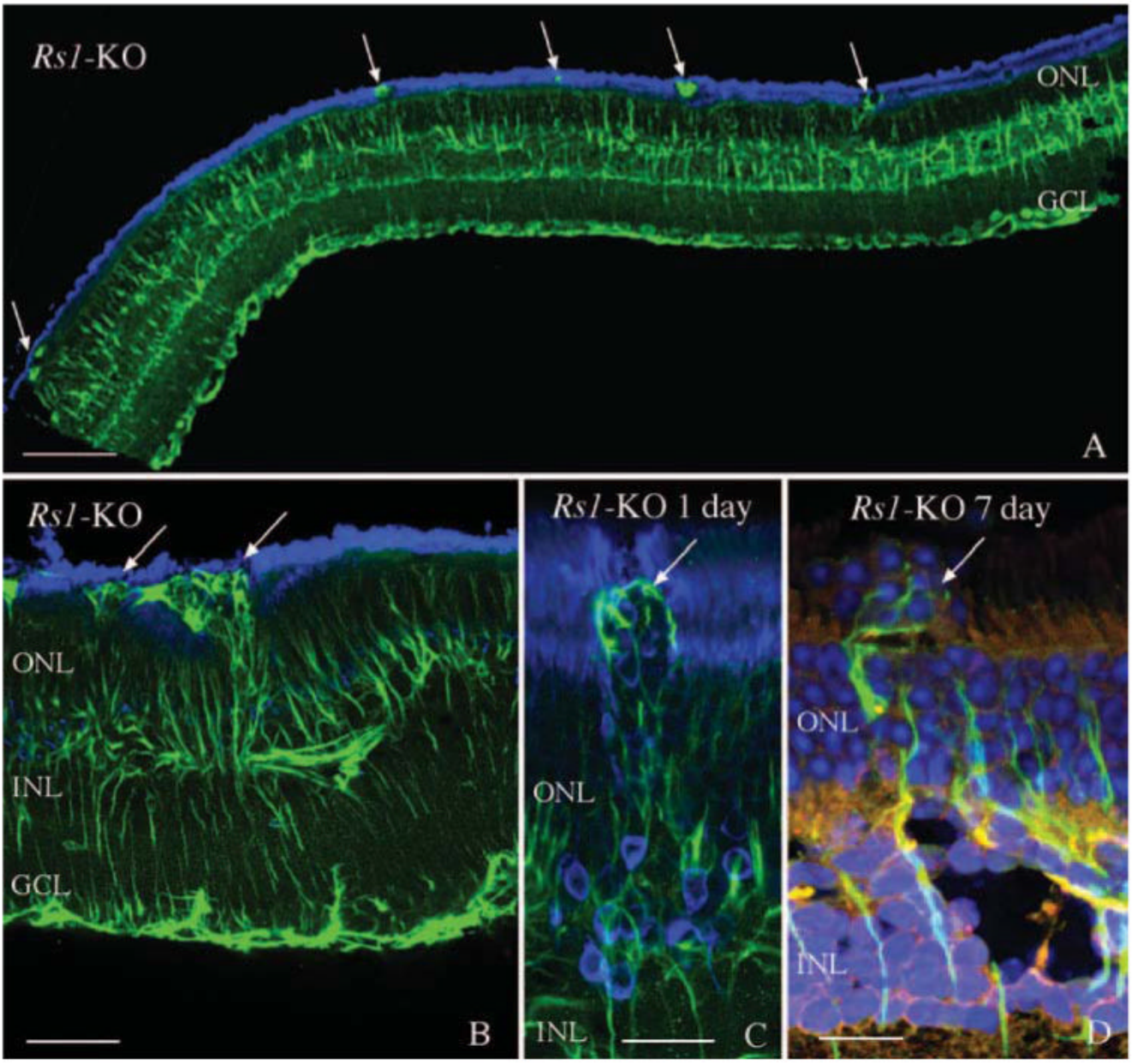

Figure 2.

Laser scanning confocal images illustrating the presence of anti-GFAP labeled processes (*green; arrows*) in the subretinal space in nondetached (**A**, **B**) and detached (**C**, **D**) *Rs1*-KO retinas. Numerous anti-GFAP–labeled glial scars were observed in *Rs1*-KO retinas before detachment (**A**, **B**; *arrows*) resulting in photoreceptor outer segment disruption. A similar pattern of subretinal glial scars was observed after detachment (**C**, **D**; *arrows*). The presence of the scars was associated with a redistribution of the rod opsin protein (*blue*) to the ONL (**C**) as well as extrusion of photoreceptor nuclei (*blue*) into the subretinal space (**D**, *arrow*). Anti-rod opsin labeling is *blue* in (**A**), (**B**), and (**C**). Hoechst labeling of nuclei is *blue* in (**D**). GCL, ganglion cell layer. Scale bars: (**A**) 100 μm; (**B**) 50 μm; (**C**, **D**) 20 μm.

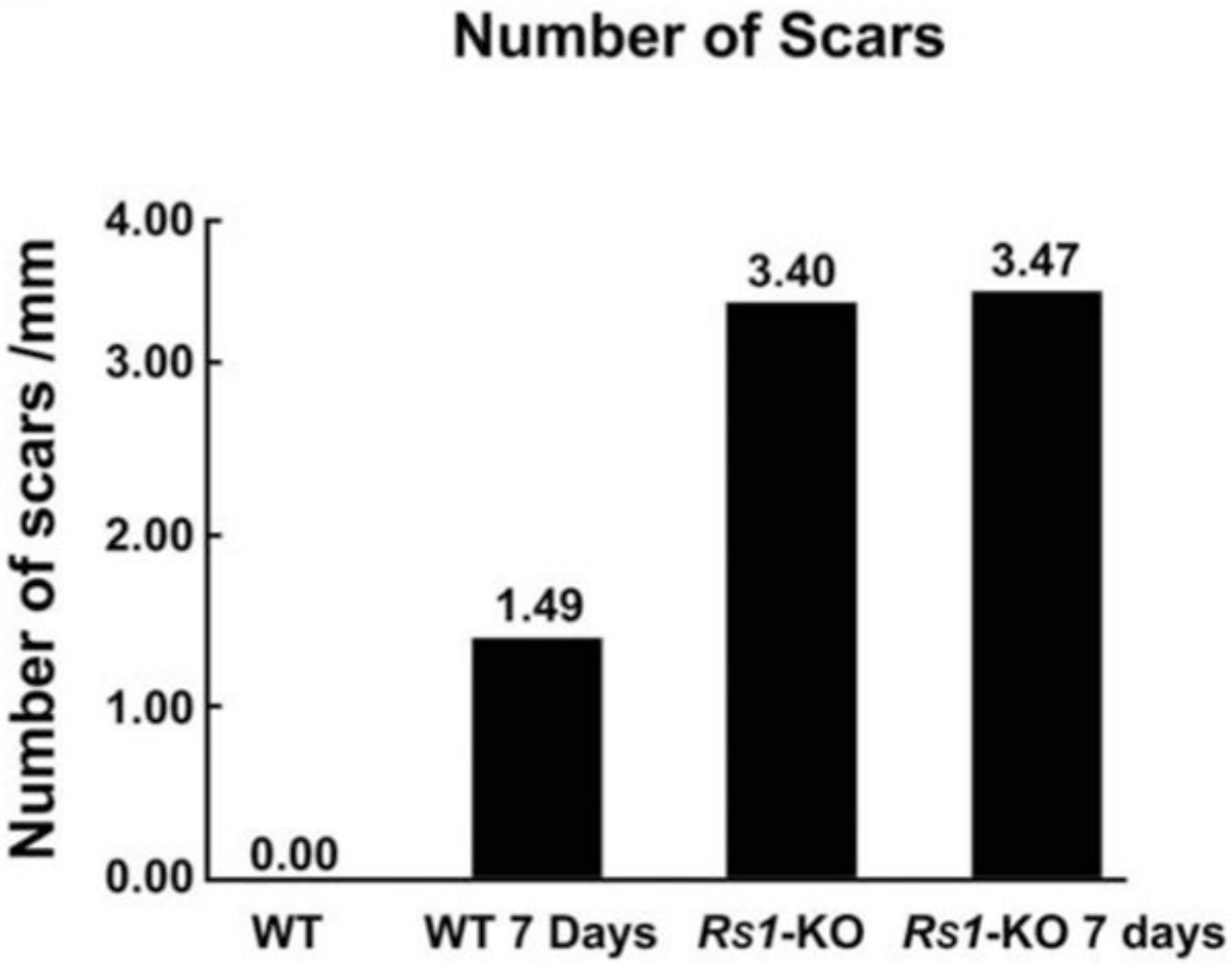

Figure 3.
Graph comparing the number of subretinal scars per millimeter of retina in wt nondetached (wt) and detached (wt 7 days) retinas, with *Rs1*-KO nondetached (*Rs1*-KO) and detached (*Rs1*-KO 7 days) retinas. (The experimental retinas were detached for 1 day and reattached 6 days for a total of 7 days.) There was a significant increase in the presence of subretinal glial scars in the nondetached *Rs1*-KO retinas compared with wt detached retinas. Detachment of the *Rs1*-KO retinas did not increase the number of scars compared with the number in the nondetached *Rs1*-KO retinas.

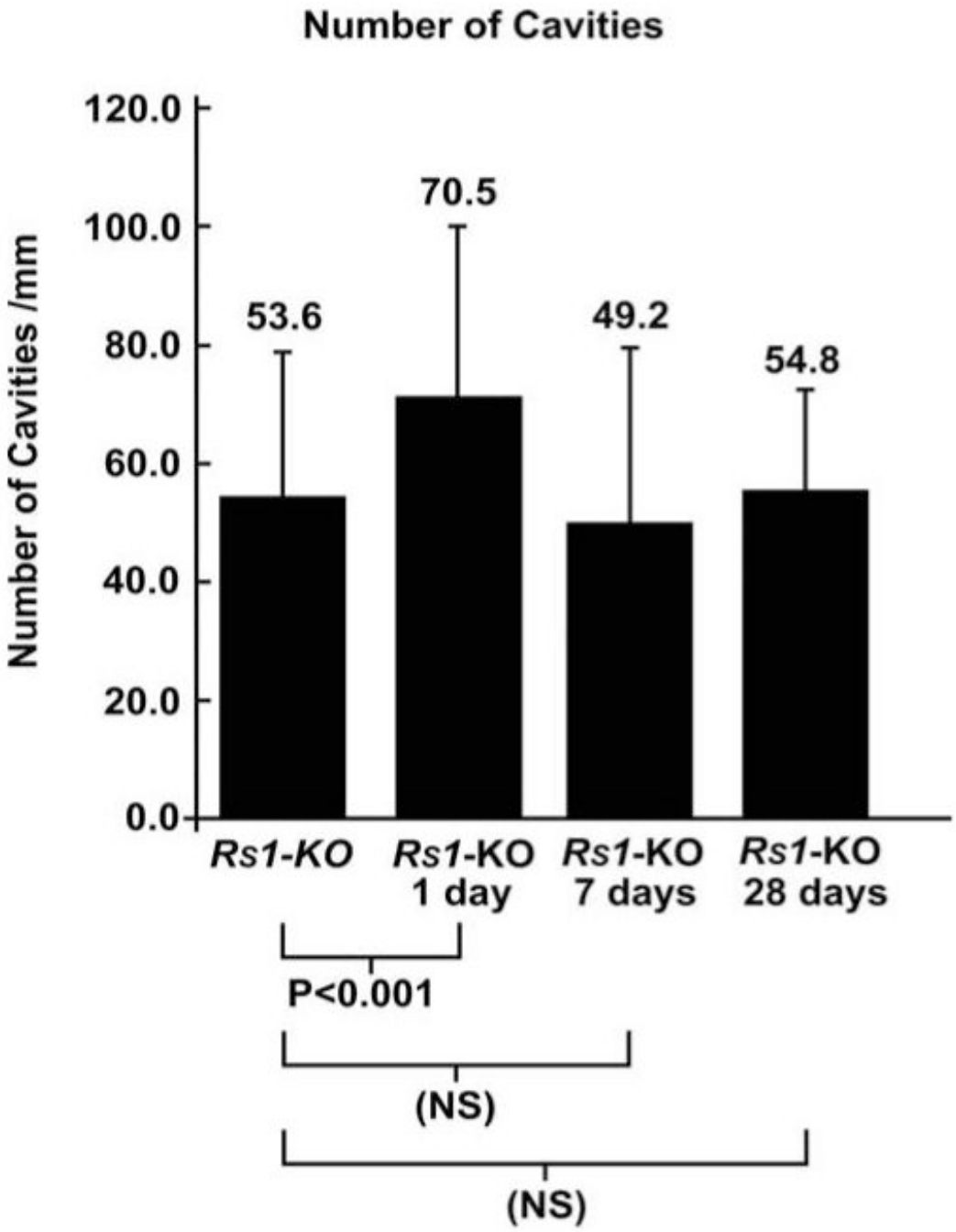

Figure 4.

Graph comparing the number of retinal cavities present in nondetached *Rs1*-KO retinas (*Rs1*-KO) with retinas detached for 1 day (*Rs1*-KO 1day), detached for 1 day and reattached for 6 days (*Rs1*-KO 7days), and detached for 1 day and reattached for 27 days (*Rs1*-KO 28 days). A slight but significant increase in the number of cavities was observed in the *Rs1*-KO 1-day retinas, but at later time-points this decreased to similar levels in the nondetached retinas. Error bars, SD.

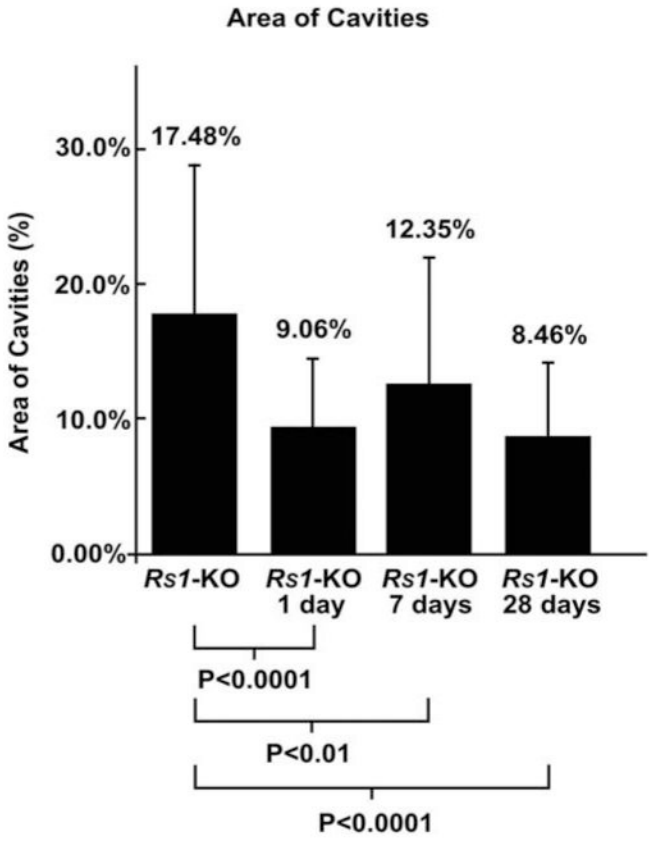

Figure 5.
Graph comparing the area of cavities in nondetached *Rs1*-KO retinas (*Rs1*-KO) with that in retinas detached for 1 day (*Rs1*-KO 1 day), detached for 1 day and reattached for 6 days (*Rs1*-KO 7 days), and detached for 1 day and reattached for 27 days (*Rs1*-KO 28 days). At all times after detachment, there was a significant decrease in the area of cavities compared with that in the nondetached retinas. Error bars, SD.

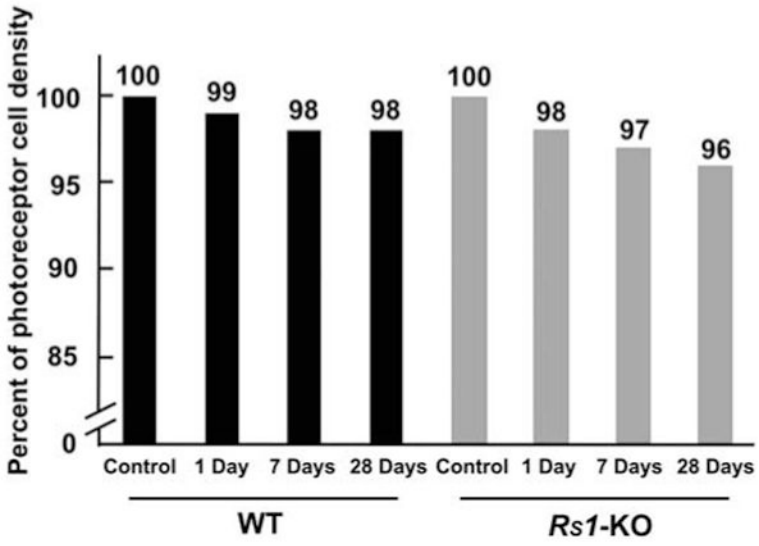

Figure 6.

Graph comparing the percentage of photoreceptor density in nondetached and detached wt and *Rs1*-KO retinas. One day, 1 day detached; 7 days, 1 day detached and 6 days reattached; 28 days, 1 day detached and 27 days reattached. The total number of photoreceptors was less in the nondetached *Rs1*-KO retinas than in the nondetached wt retinas. Detachment produced a slight but steady decline in the number of photoreceptors in both sets of animals. The decrease in the density of photoreceptors by 28 days in the *Rs1*-KO detachments was statistically significant.

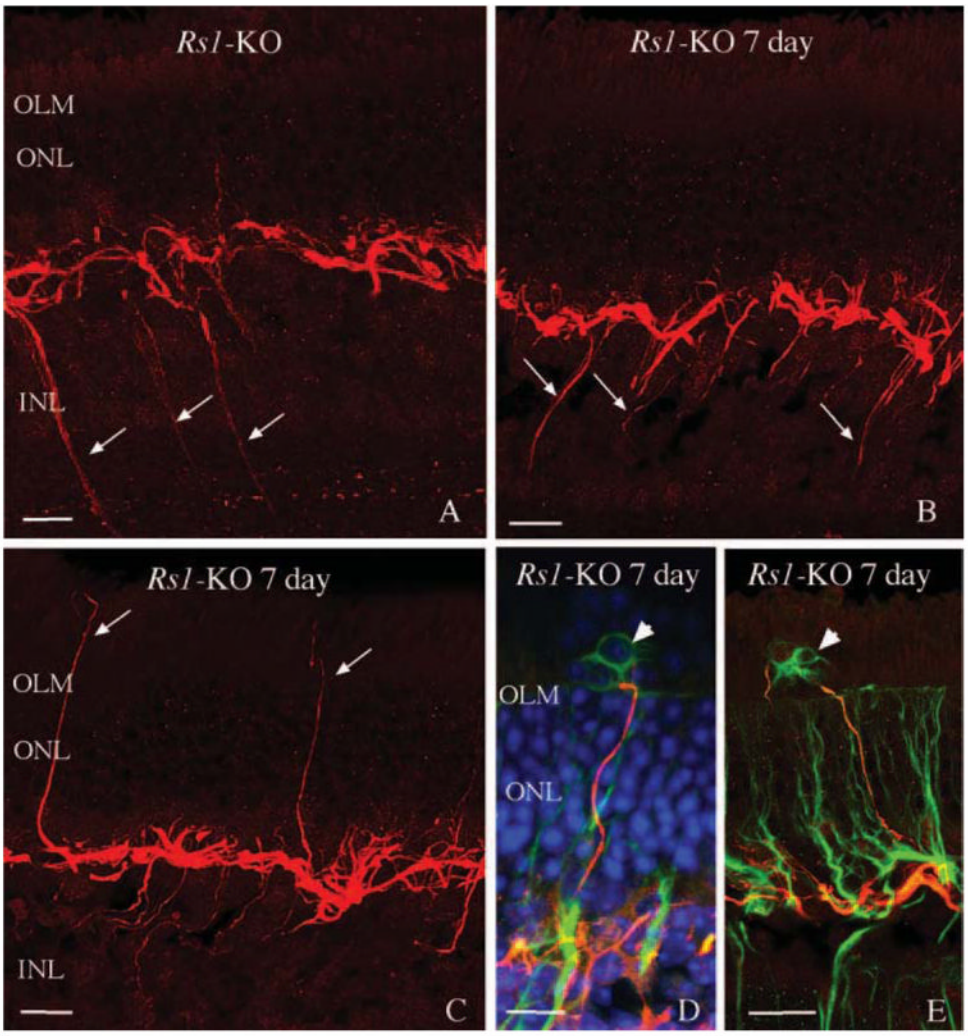

Figure 7.

Laser scanning confocal images illustrating the neurite outgrowth from horizontal cells in nondetached (**A**) and detached (**B–E**) *Rs1*-KO retinas at day 7 (i.e., 1 day detached, 6 days reattached). Anti-neurofilament-labeled (*red*) processes originating from horizontal cells (*arrows*), extending into the inner retina in nondetached retinas (**A**) and detached retinas (**B**), as well as into the outer retina in both nondetached and detached conditions (**C–E**; 1 day detached, 6 days reattached). Neurites can be observed in the subretinal space but only in regions with anti-GFAP-labeled glial scars (*green; arrowheads*). *Blue*: Hoechst-labeled nuclei. OLM, outer limiting membrane. Scale bars, 20 μm.